Heliyon 10 (2024) e31617

Contents lists available at ScienceDirect

Heliyon

journal homepage: www.cell.com/heliyon

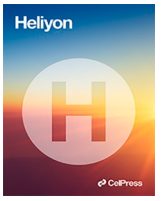

Research article

Ampicillin detection using absorbance biosensors utilizing Mn-doped ZnS capped with chitosan micromaterials

Son Hai Nguyen [a], Van-Nhat Nguyen [b], Mai Thi Tran [b,c,*]

[a] School of Mechanical Engineering, Hanoi University of Science and Technology, Hanoi, 100000, Viet Nam
[b] College of Engineering and Computer Science, VinUniversity, Hanoi, 100000, Viet Nam
[c] VinUni-Illinois Smart Health Center, VinUniversity, Hanoi, 100000, Viet Nam

ARTICLE INFO

Keywords:
Zinc sulphide
Chitosan
Ampicillin
Sensors
Absorbance

ABSTRACT

The detection of ampicillin plays a crucial role in managing and monitoring its usage and resistance. This study introduces a simple and effective biosensor for ampicillin detection, utilizing the unique absorbance features of Mn-doped ZnS capped by chitosan micromaterials in conjunction with β-lactamase activity. The biosensors can detect ampicillin concentrations from 13.1 to 72.2 μM, with a minimum detection limit of 2.93 μM for sensors based on 300 mg/L of the sensing material. In addition, these sensors show high specificity for ampicillin over other antibiotics such as penicillin, tetracycline, amoxicillin, cephalexin, and a non-antibiotic-glucose. This specificity is demonstrated by an enhancing effect when beta-lactamase is used, as opposed to a quenching effect observed at 340 nm in the absorbance spectrum when no beta-lactamase is present. This research highlights the potential of affordable chitosan-capped Mn-doped ZnS micromaterials for detecting ampicillin through simple absorbance measurements, which could improve the monitoring of antibiotics in both clinical and environmental settings.

1. Introduction

Ampicillin, once hailed as a groundbreaking antibiotic in treating various bacterial infections, has seen its ubiquity extend beyond medical applications [1]. The increasing use of antibiotics like ampicillin in agriculture and aquaculture has raised concerns about drug residues in milk, food, and water systems [2,3]. The prevalence of ampicillin in these environments not only presents potential direct health implications but also indirectly exacerbates the menace of antimicrobial resistance (AMR) [4,5]. Over time, extensive research has been dedicated to monitoring ampicillin levels in different food sources and water bodies and establishing maximum residue limits (MRLs) to ensure consumer safety [6]. Concurrently, there is growing emphasis on developing rapid and precise detection methods for ampicillin residues.

Identifying low levels of ampicillin in complex samples can be complicated by the presence of other substances that may mask the target analyte, necessitating methods with both high sensitivity and specificity. Conventional techniques for detecting ampicillin, such as Microbial Assays, Enzyme-Linked Immunosorbent Assay, Liquid Chromatography Mass Spectrometry and High-Performance Liquid Chromatography, are developed to address these challenges [7–10]. While these traditional methods are effective, they often demand complex equipment, specialized staff, and sample pre-treatment, which hampers their application to detect real-time or on-site. Nano/micromaterial-based optical sensors are gaining attention to detect ampicillin and other substances for several reasons [11,

* Corresponding author. College of Engineering and Computer Science, VinUniversity, Hanoi, 100000, Viet Nam.
E-mail address: mai.tt@vinuni.edu.vn (M.T. Tran).

https://doi.org/10.1016/j.heliyon.2024.e31617
Received 29 February 2024; Received in revised form 18 May 2024; Accepted 20 May 2024
Available online 21 May 2024

12]. The unique optical properties of nano/micromaterials can lead to enhanced signal intensities, allowing for the detection of low concentrations of ampicillin. Some nanomaterial-based sensors allow for immediate or real-time detection, which is valuable in many practical scenarios [13]. Nanomaterials can be functionalized with various molecules to achieve specificity towards specific compounds, making them adaptable for diverse applications [14]. Although initially expensive, the scalability and potential for producing portable devices may render micromaterial-based sensors cost-effective in the long run.

In the past decade, numerous studies have explored the application of optical biosensors based on nano-micromaterials for antibiotic detection. For instance, fluorescent biosensors utilizing quantum dots have been reported to detect antibiotics like tetracycline and sulfamethazine [15,16]. Similarly, utilizing the localized surface plasmon resonance properties, colorimetric biosensors made from gold nanoparticles are commonly used, enabling the detection of antibiotics such as penicillin and chloramphenicol [17,18]. Moreover, there have been reports on using photonic crystals and up-conversion nanoparticles in developing optical biosensors for antibiotics, highlighting the broad spectrum of nanomaterials that can be utilized [19]. Despite these advantages, the field of optical nano and micromaterial-based biosensors for antibiotics is still developing. There is substantial scope for designing sensors based on different materials to enhance sensitivity, specificity, detection range, and limit of detection, all while reducing costs and simplifying preparation processes. Recent advancements in biosensing and analytical detection have seen significant attention given to utilizing Mn-doped ZnS materials, particularly for antibiotics detection, including ampicillin [20–22]. Chitosan, a biocompatible and biodegradable polymer, enhances the stability and dispersibility of the materials in aqueous environments, ensuring consistent optical properties while minimizing non-specific interactions [23]. Hence, chitosan capped on Mn-doped ZnS materials will stabilize Mn-doped ZnS [24]. Furthermore, exposure to analytes leads to molecular-level interactions between the molecules and the chitosan-capped Mn-doped ZnS, resulting in measurable changes in the absorbance of the sensors [25,26]. This measurable change in real-time can detect and quantify analytes' concentrations, which is crucial for monitoring drug therapy and assessing antibiotics's presence.

In this study, the sensitivity and stability of the sensing materials are enhanced by enzyme reactions in the sensing platform. Enzymes, known for their catalytic abilities and substrate specificity, offer a reliable method to identify the quantity and presence of antibiotics. In addition, the proposed sensors can differentiate ampicillin (AMP) from different selected analytes, including glucose, amoxicillin (AMX), cephalexin (CEX), penicillin G (PCN), and tetracycline (TET). This study aims to establish a straightforward and effective biosensing platform to identify and measure AMP with exceptional sensitivity and specificity using absorbance measurements. Although there are numerous AMP sensors, they typically exhibit higher detection limits. They are often based on complex and expensive production processes, or they employ a range of detection techniques that may be less practical. A comparison of the performance of our proposed sensor with these sensors is presented in Section 3. This document presents a proof-of-concept for a biosensor developed to detect AMP concentrations between 13.1 and 72.2 μM. This study presents the first report of an AMP absorbance biosensor utilizing Mn-doped ZnS capped with chitosan microparticles.

2. Methods

2.1. Chemicals

Zinc acetate dihydrate ($Zn(CH_3COO)_2{\cdot}2H_2O$) and manganese chloride tetrahydrate ($MnCl_2{\cdot}4H_2O$) were purchased from Merck, Germany. Sodium sulfide nonahydrate ($Na_2S{\cdot}9H_2O$, 98 % purity), and ethanol (C_2H_5OH, 99.5 % purity) were obtained from Xilong Scientific Co., Ltd. Chitosan ($C_6H_{11}NO_4$, 90 % purity) and β-lactamase ($C_{21}H_{17}N_3O_8S_3$, CAS # 9073-60-3, purity ≥95 %) were produced from Shanghai Zhanyun Chemical Co., Ltd. and Shanghai Yuanye Bio-Technology Co., Ltd, respectively. D-Glucose monohydrate ($C_6H_{12}O_6{\cdot}H_2O$, 99.99 % purity) and Tetracycline hydrochloride ($C_{22}H_{24}N_2O_8{\cdot}HCl$, ultra-pure) were purchased from Biobasic, Ontario, Canada. Amoxicillin crystalline ($C_{16}H_{19}N_3O_5S$, 99 % purity) and cephalexin monohydrate ($C_{16}H_{19}N_3O_5S{\cdot}H_2O$, 98 % purity) were bought from Shanghai Macklin Biochemical Co., Ltd. Ampicillin sodium salt ($C_{16}H_{18}N_3NaO_4S$, 99.99 % purity and Penicillin G sodium salt ($C_{16}H_{17}N_2NaO_4S$, Ultra-pure) were obtained from Njduly and Bomeibio, China, respectively.

2.2. Sensing micromaterial preparation

The ZnS doped Mn and capped by chitosan ((Mn: ZnS)CH) materials were synthesized via the hydrothermal method, following the procedure detailed in Ref. [27]. First, 7.32 g of $Zn(CH_3COO)_2$ and 0.08 g $MnCl_2$ were added to 80 mL deionized water (DI), and the mixture was stirred until it completely dissolved to form Suspension 1. Subsequently, Suspension 2 was prepared by mixing 0.6 g chitosan with 40 mL of 1 % acetic acid. Suspension 1 was then gradually added to Suspension 2, along with 3.12 g of Na_2S. This mixture was stirred for 1 h and then placed in a Teflon autoclave. This hydrothermal process occurred for 2 h at 80 °C. Afterward, the precipitate was washed and centrifuged several times with ethanol. Finally, the resulting materials were completely dried for 7 h at 60 °C. For comparison, ZnS and Mn-doped ZnS materials were also synthesized using a similar methodology, except Suspension 2 was not prepared in these cases. Suspension 1 consisted of $Zn(CH_3COO)_2$ dissolved in 80 mL of DI for ZnS synthesis. The solvent used in all experiments was deionized water unless noted otherwise.

2.3. Absorbance detection setups and measurements

Both pure antibiotics and antibiotics treated by beta-lactamase were examined in this study. Analytes were mixed with the β-lactamase enzyme in equal proportions and adjusted to the necessary concentrations before experimentation. These blends were then

kept at 3 °C. Prior to use, the pH levels of all samples were confirmed and noted as follows: ZnS (6.24), (Mn: ZnS) (6.53), (Mn:ZnS)CH (6.06), Glucose (3.78), Glucose-Enzyme (6.11), AMP (7.48), AMP-Enzyme (7.97), PCN (5.06), PCN-Enzyme (6.63), TET (2.53), TET-Enzyme (2.89), AMX (5.91), AMX-Enzyme (6.12), CEX (5.26), and CEX-Enzyme (5.58).

In our experiment, 1500 μL of sensing materials at a specific concentration were initially introduced into cuvettes. Then, 100 μL increments of the analyte were added to adjust the concentration levels from 13.1 to 72.2 μM. We measured the absorbance at each concentration using a DS-11 FX + DeNovix UV–visible spectrometer. To further investigate the dependency of sensing performance on sensing concentrations, (Mn:ZnS)CH was prepared in deionized water at concentrations of 300, 524, 800, and 1000 mg/L. These solutions were then exposed to pure AMP and AMP treated with the enzyme to examine their interactions.

3. Results and discussions

3.1. Synthesized material's characterizations

Fig. 1(a) shows XRD patterns with three notable peaks at the (111), (220), and (311) positions, corresponding to 2θ angles of 28.9°, 48.4°, and 57.3°, respectively. These peaks verify that ZnS has been successfully synthesized with the cubic sphalerite structure, as indexed by JCPDS card No.5-0566. The inclusion of Mn^{2+} and chitosan has a negligible impact on the ZnS structure, probably due to their minimal concentrations. Additionally, Fig. 1(b) presents an SEM image with the microparticle morphology of the sensing material, with average sizes ranging from 0.2 to 0.5 μm.

3.2. Absorbance biosensors utilizing (Mn: ZnS)CH micromaterials

3.2.1. Absorbance biosensors to indirectly detect ampicillin

First, the biosensors were exposed to deionized water and pure AMP. The absorbance spectra are shown in Fig. 2(a and b). These preliminary tests revealed a decrease in absorbance levels, with nearly identical slopes observed in both experiments. Therefore, initially, the proposed sensors could not directly detect AMP. However, by incorporating β-lactamase, an enzyme that interacts specifically with β-lactam antibiotics like AMP, we can take advantage of this interaction. The enzyme breaks down the β-lactam ring in ampicillin, changing its molecular configuration. This enzymatic activity generates a measurable signal for biosensors. Sensors with (Mn: ZnS)CH thus indirectly measure AMP by detecting its degradation products formed during the β-lactamase processing (AMP-Enzyme). Fig. 2(c) shows the absorbances of these sensors interacting with the AMP-Enzyme complex at AMP concentrations from 13.1 to 72.2 μM. AMP treated β-lactamase enhanced the absorbances of proposed sensors in the 308–372 nm range, with a peak at 340 nm. This phenomenon proves that the byproducts of the reaction between AMP and beta-lactamase play key roles in this increase. Although the absorbance of AMP-Enzyme itself increased with the concentration (Fig. 2(d)), this change was minimal, from 0.01 to 0.045 for concentrations of 13.1–72.2 μM at the absorbance peak at 340 nm. Hence, we can confirm that our proposed sensors are effective, and the absorbance at 340 nm can be used to evaluate the working performance of sensors. The absorbances changed at 340 nm with the concentrations of analytes displayed in Fig. 2(e). The absorbances of (Mn: ZnS)CH increased linearly with the concentrations of AMP-Enzyme. Hence, AMP concentrations ranging from 0 to 72.2 μM can be estimated using the linear function ($R^2 = 0.996$):

$$y = 0.00407x + 0.222, \tag{1}$$

where y denotes the absorbance at 340 nm, x presents the AMP concentration (μM) prior to its introduction into the beta-lactamase solution.

In a further step, we prepared four test samples with known concentrations within the testing range and measured the absorbances at 340 nm for each. By substituting the measured absorbance value into Equation (1), we can calculate the concentrations of samples. The results, shown in Table 1, indicate that differences between actual and estimated concentrations were smaller than 10 % for all

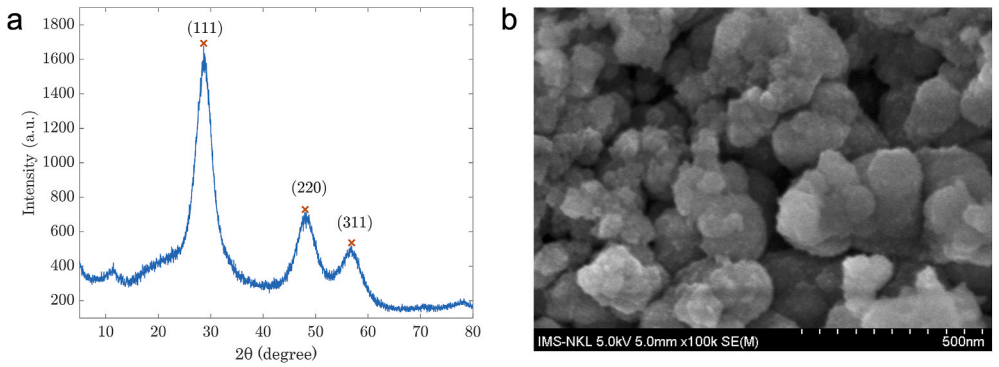

Fig. 1. Properties of the synthesized materials. (**a**) X-ray diffraction (XRD) patterns. (**b**) Scanning Electron Microscopy (SEM) image of the Mn-doped ZnS capped by chitosan material.

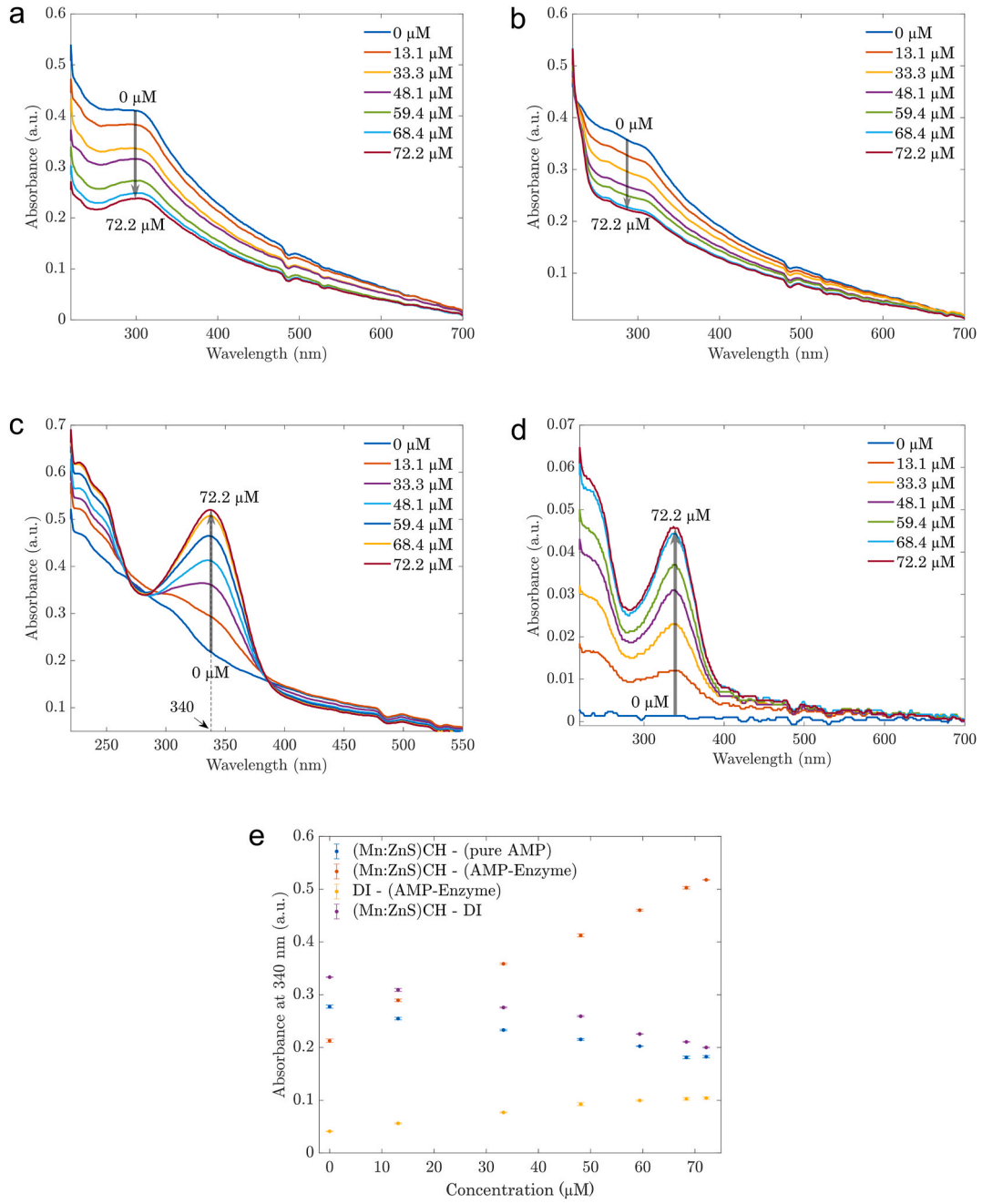

Fig. 2. Absorbance spectra depicted in the figure feature: (**a**) sensors developed from 524 mg/L (Mn:ZnS)CH micromaterials, diluted with varying volumes of deionized water, each volume representing a different antibiotic concentration as indicated in the legends, (**b**) these sensors after exposure to different concentrations of AMP, (**c**) sensors interacting with AMP-enzyme complexes, with legends indicating the initial AMP concentrations before beta-lactamase treatment, (**d**) various concentrations of the AMP-enzyme complex, and (**e**) absorbance shifts at a 340 nm wavelength for different concentrations of analytes (DI, AMP, AMP-Enzyme). Error bars indicate standard deviations from nine measurements.

cases, with the difference decreasing as the test sample concentration increased.

3.2.2. Effect of (Mn:ZnS)CH concentrations on the performance of the absorbance biosensor

As demonstrated in the previous section, sensors utilizing (Mn: ZnS)CH can detect ampicillin after it has been modified by the beta-lactamase. This section assesses the sensitivity of AMP sensors across a range of sensing material concentrations. Biosensors were set up with (Mn: ZnS)CH microparticle concentrations from 300 mg/L to 1000 mg/L, while AMP concentrations varied between 13.1 and 72.2 μM. Initially, absorbances were recorded before the sensors interacted with the AMP-Enzyme. Fig. 3(a) shows the absorbance

Table 1
Validation of our proposed sensors based on Equation (1).

Sample concentration (μM)	Absorbance at 340 nm (a.u.)	Estimated concentration (μM)	Difference (%)
24.05	0.33	25.83	7.38
41.23	0.38	39.80	3.46
54.11	0.44	53.21	1.67
64.13	0.48	63.31	1.29

profiles at four different (Mn: ZnS)CH microparticle levels. The results illustrated that the sensor's absorbance was enhanced when the sensing materials' concentration increased. Then, four sensors were exposed to different AMP-Enzyme concentrations. The 300 mg/L based sensors showed an enhancing effect across all wavelengths (Fig. 3(b)), while both quenching and enhancing effects were observed for sensors with higher concentrations of sensing materials (Fig. 3(c–e)). The plots indicate that with four concentrations of the sensing materials, the enhancing effects occurred within the bandwidth from 308 to 372 nm and the enhancing peaks at 340 nm. Based on the absorbances of sensors at 340 nm, the sensors' responses to various AMP concentrations are displayed in Fig. 3(f). All responses of different sensors can be fitted linearly with high precisions and summarized in Table 2. As indicated in Table 2, sensors utilizing 300 mg/L of (Mn: ZnS)CH microparticles are preferred due to their high sensitivity (slope of 0.0055) and precision (R^2 = 0.998), along with a low limit of detection (2.93 μM, calculated using the S/N = 3 method, where LOD = blank signal + 3 standard deviations).

3.2.3. The specificity and stability of absorbance biosensors to different analytes

To evaluate the specificity of the proposed sensor, detection experiments were conducted under identical conditions with various analytes: different β-lactam antibiotics (penicillin G- PCN, Amocixillin- AMX, and Cephalexin- CEX), a non β-lactam antibiotic (Tetracycline – TET), and a non-antibiotic substance (glucose). Each analyte was examined in its pure form and after treatment with beta-lactamase, similar to the approach used with AMP. The absorbance measurements of the sensors in the presence of these analytes are shown in Supplement S1.

The data in Supplement S1 reveal distinct absorbance spectra of the sensors when exposed to different analytes, enabling the differentiation of AMP from the six tested analytes. Specifically, both TET and TET-Enzyme exhibited enhancing effects with peaks at 275 nm and 360 nm, and the absorbance changes for these two cases were nearly identical. In contrast, only AMP-Enzyme generated an enhancing absorbance effect within the resonant band from 308 nm to 372 nm, featuring a peak at 340 nm. For all other analytes tested, increasing their concentration resulted in a decrease in absorbance. The distinctive enhancing effect with a single peak at 340 nm uniquely identifies AMP among the tested analytes and can be used for quantifying unknown AMP concentrations.

To further illustrate the specificity of our sensors, the absorbance responses to various analyte concentrations at 340 nm are depicted in Fig. 4(a and b). While TET and TET-Enzyme showed higher positive slopes with almost identical values, the unique positive slope of AMP-Enzyme confirmed the enhancement phenomenon in the absorbance, distinguishing it from other analytes (Fig. 4(b)). PCN, PCN-Enzyme, and glucose exhibited quenching effects characterized by negative slopes. These results are based on the average of nine measurements, with the concentration of (Mn: ZnS)CH microparticles set at 524 mg/L.

The high specificity of the proposed sensor is achieved due to the unique properties of beta-lactamase and the structure of the sensing material. The enzyme is recommended to operate at 37 °C and a pH of 7.4. However, we tested the proposed sensors at room temperature, and they performed effectively at a pH of 6.06. The pH values of all analytes were measured and shown in the Methods section. A combination of (Mn: ZnS)CH and AMP- Enzyme resulted in a suspension with a pH of 7.02 at room temperature, the only sample exhibiting a pH greater than 7. Since TET lacks a β-ring, the enzyme does not impact this antibiotic, which is similar to the non-antibiotic of glucose. Therefore, the observed enhancement effect on the sensor's absorbance is solely attributed to the byproducts of AMP-Enzyme.

Fig. 5 depicts the schematic demonstrating the operating principle of the proposed sensors for detecting AMP. The enhancement effect of these sensors on the AMP-Enzyme interaction is explained as follows. The β-lactamase enzyme breaks down the β-ring of AMP, producing penicilloic acid and ion H^+ [28]. The hydrolyzed byproducts from AMP and β-lactamase enzyme interact with chitosan-capped (Mn:ZnS) microparticles. Chitosan's hydroxyl amino groups are crucial due to their reductive properties, which aid in microparticle formation and enable bonding via electrostatic forces, hydrogen bonds, or covalent connections with these byproducts [29,30]. These byproducts likely attach to the (Mn: ZnS)CH surface, altering its dielectric properties. Furthermore, the observed UV–Vis absorption spectra result from shifts in the energy levels of valence electrons within the molecules. Consequently, the nature of these spectra is influenced by the characteristics of the valence electrons [31]. As a result, the absorbance increases in the 308–372 nm range with the byproduct concentrations, and indirectly with the AMP concentrations. On the other hand, if the byproducts or analytes cannot bind to the (Mn: ZnS)CH micromaterials, adding more analytes is akin to lowering the concentration of sensing materials. Hence, the absorbance is diminished, as the experimental results show quenching effects for analytes other than AMP when treated with the β-lactamase enzyme.

To verify this hypothesis, we synthesized Mn: ZnS and ZnS materials using the same methods and conducted comparative experiments to evaluate their effectiveness against (Mn: ZnS)CH. The structures and morphologies of these materials were verified through XRD and SEM images in Supplement S2. Fig. 6 presents the absorbance spectra for (Mn: ZnS) (Fig. 6(a and b)) and ZnS (Fig. 6(c and d)) when exposed to AMP and AMP-Enzyme, respectively. The data demonstrate that the presence of the enzyme does not significantly alter the absorbance spectra of these sensors.

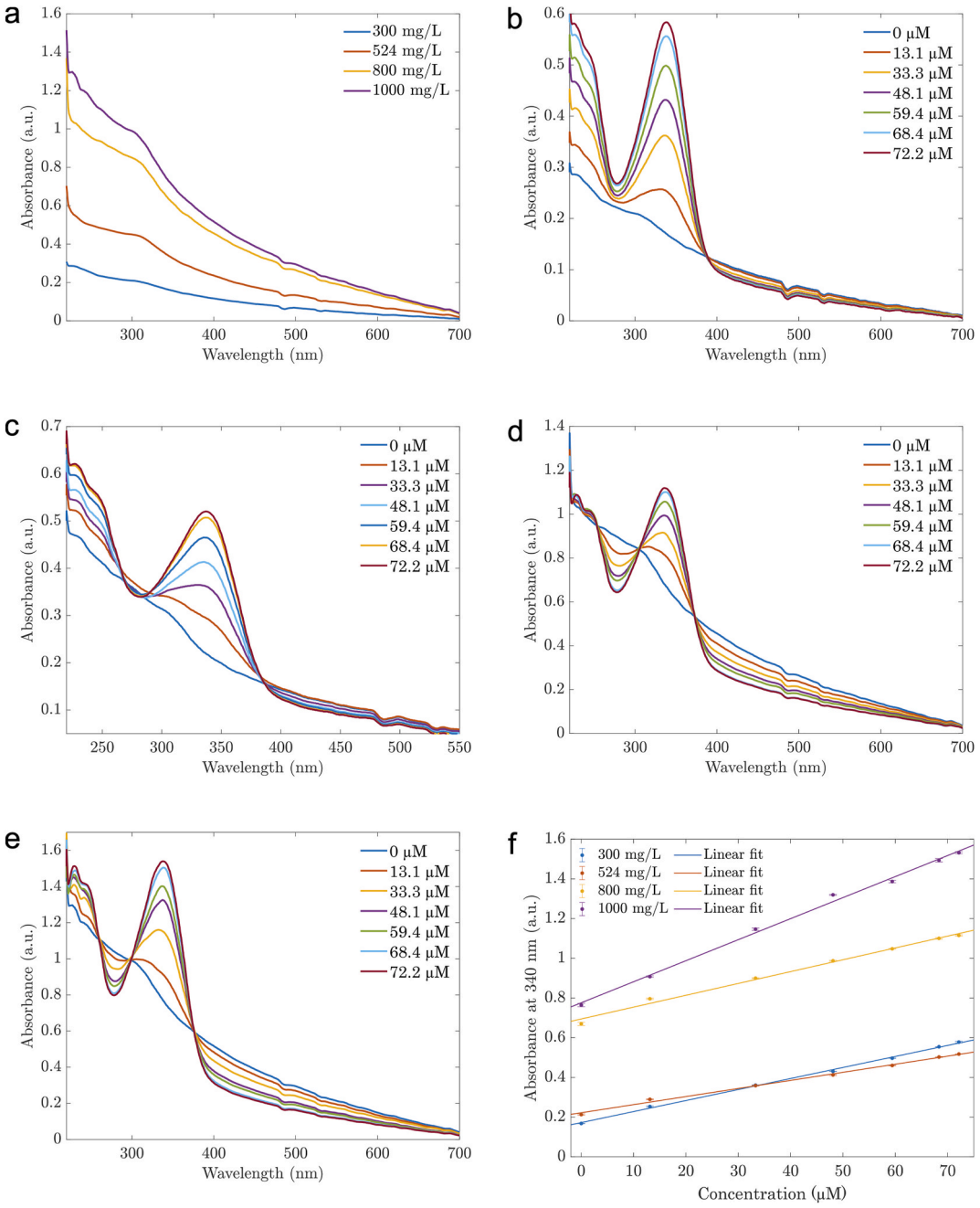

Fig. 3. The absorbance spectra of AMP sensors, prepared with different sensing material concentrations: (**a**) Before adding AMP-Enzyme, (**b**) 300 mg/L based sensors when contacting with different AMP-Enzyme concentrations, (**c**) 524 mg/L based sensors when contacting with different AMP-Enzyme concentrations, (**d**) 800 mg/L based sensors when contacting with different AMP-Enzyme concentrations, (**e**) 1000 mg/L when contacting with different AMP-Enzyme concentrations, (**f**) The relationship between the absorbances of the biosensors at 340 nm with different concentrations of (Mn: ZnS)CH and AMP-Enzyme concentrations. Error bars depict standard deviations based on nine measurements.

To elucidate the performance differences among the three sensor types, we examined how absorbance at 340 nm varied with the concentration of analytes. These absorbance changes and the absorbance difference ΔI (%) at 340 nm are shown in Fig. 7. Both (Mn: ZnS) and ZnS-based-sensors exhibited similar responses to AMP, whether in its pure form or treated with the enzyme. At 340 nm, ZnS-based sensors showed a slight enhancing effect (Fig. 7(a)). However, the absorbance changes were not linearly correlated with AMP concentrations and remained minimal, ranging from 0.05 to 0.15. The negligible initial absorbance led to significant increases in the absorbance difference ΔI for ZnS-based sensors (210 %) (Fig. 7(b)). (Mn: ZnS)CH was the only material that clearly differentiated between AMP with and without enzyme. The results indicate the critical role of chitosan in facilitating this phenomenon and support

Table 2
The fitting functions of different sensors based on the experimental data in Fig. 3(f).

Concentration of (Mn: ZnS)CH (mg/L)	Operating function	R^2	Limit of detection (μM)
300 μM	$y = 0.0055x + 0.1725$	0.998	2.93
524 μM	$y = 0.0041x + 0.2220$	0.996	4.82
800 μM	$y = 0.0060x + 0.6944$	0.992	6.55
1000 μM	$y = 0.0106x + 0.7760$	0.996	4.66

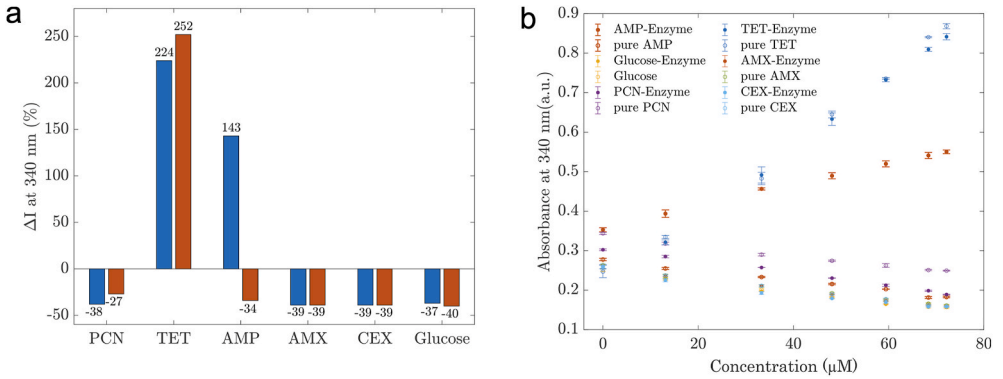

Fig. 4. Illustration of the high specificity of (Mn:ZnS)CH based sensors. (**a**) The histograms of absorbance difference at 340 nm ΔI between samples with 0 and 72.2 μM of the analyte added, (**b**) The absorbance at 340 nm changed with the concentrations of analytes from 0 to 72.2 μM.

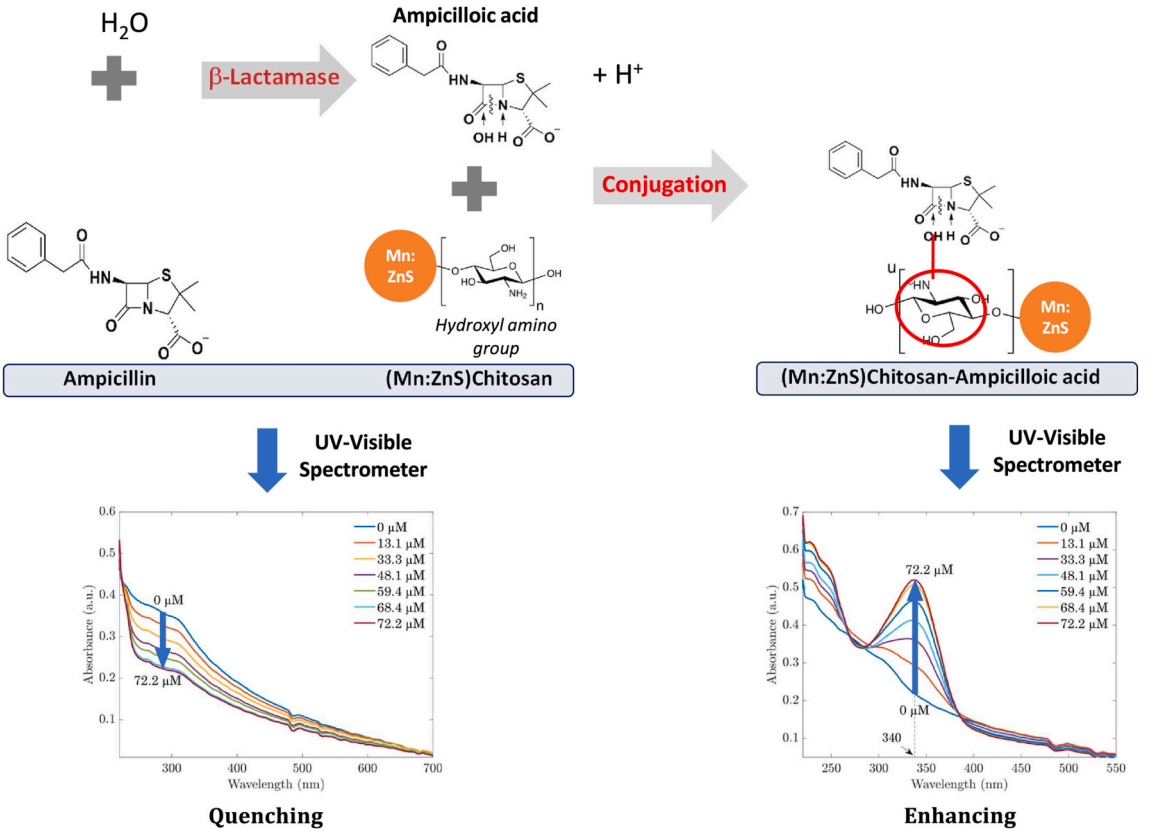

Fig. 5. The operational mechanism of the proposed sensors for detecting AMP.

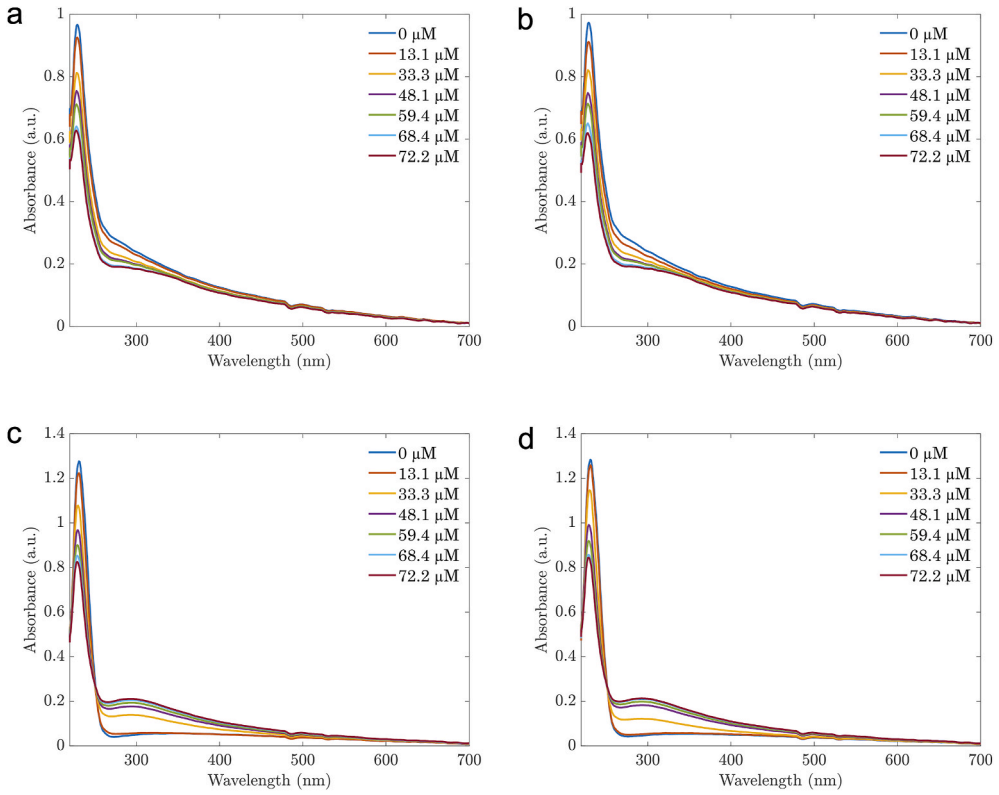

Fig. 6. Absorbance profiles for various sensors: (**a**) (Mn: ZnS)-based sensors interacting with AMP-Enzyme, (**b**) (Mn: ZnS)-based sensors exposed to AMP, (**c**) ZnS-based sensors interacting with AMP-Enzyme, (**d**) ZnS-based sensors exposed to AMP.

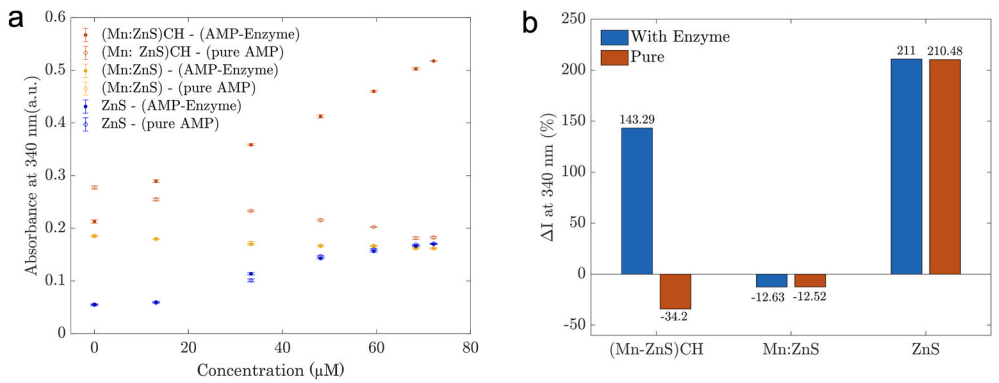

Fig. 7. Comparison of three sensor types' performance: (**a**) Correlation between the 340 nm absorbance and analyte concentrations for sensors based on ZnS, ZnS doped – Mn, and ZnS doped Mn capped by chitosan. (**b**) The absorbance difference at 340 nm for sensors with and without the enzyme.

our hypothesis above.

To assess the stability of the sensors, they were maintained at room temperature, and samples were preserved at 3 °C. The experiments with absorbance sensors were conducted every 7 days over a month. The results, shown in Fig. 8, demonstrate the long-term stability of the sensors.

This study presents a new and cost-effective (Mn: ZnS)CH-based absorbance sensor for detecting AMP, which is noted for its high sensitivity, stability, and specificity. Although numerous AMP sensors have been reported, these alternatives often exhibit higher limits of detection (LODs) or rely on more complex and expensive fabrication methods or different detection approaches. For example, Hamami utilized a MoS_2/PPy nanocomposite as a transducer in electrochemical aptasensors to detect AMP in river water, achieving a LOD of 0.28 pM [32]. Lin and Cen developed an absorbance sensor that can detect AMP concentrations ranging from 17.47 to 69.88 mg/L, with a detection limit of 0.52 mg/L by monitoring AMP degradation under alkaline conditions [33]. Garcia-Zamora created

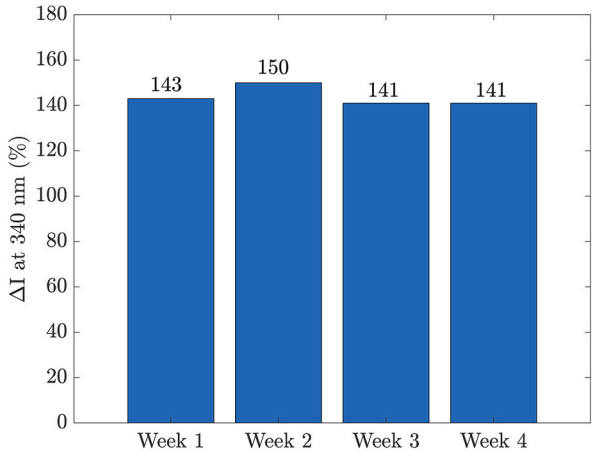

Fig. 8. The proposed sensors exhibited high stability over four weeks.

fluorescence sensors capable of identifying AMP concentration from 0.035 to 40 μM, with a 0.026 μM LOD, by utilizing the byproducts of biocatalysis [34]. Shayesteh and Ghavami introduced colorimetric AMP aptasensors using gold nanoparticles, which can detect AMP concentrations in the 1–600 nM range and feature an LOD of 0.1 nM [35]. Lastly, Youn et al. reported on an aptasensor for AMP detection that is conjugated with Cyanice, 6-carboxyfluorescein, and graphene and utilizes fluorescence resonance energy transfer with a LOD of 2.337 ng/mL [36].

4. Conclusions

In summary, this research demonstrates the effectiveness of biosensors utilizing Mn-doped ZnS capped with chitosan micromaterials for detecting AMP. When treated with β-lactamase enzyme, AMP was detected with remarkable precision and sensitivity through simple absorbance measurements. These sensors exhibited excellent accuracy and durability, effectively quantifying AMP in concentrations ranging from 13.1 to 72.2 μM and achieving an impressive detection limit of 2.93 μM at a material concentration of 300 mg/L. The result represents a significant advancement for absorbance-based biosensors. With their ability to detect minute quantities of AMP, these sensors have great potential for applications in food safety, healthcare, and environmental monitoring.

Data availability statement

All data are included in the manuscript and the supplementary information.

CRediT authorship contribution statement

Son Hai Nguyen: Writing – review & editing, Writing – original draft, Visualization, Validation, Methodology, Investigation, Funding acquisition, Formal analysis, Conceptualization. **Van-Nhat Nguyen:** Data curation. **Mai Thi Tran:** Writing – review & editing, Writing – original draft, Validation, Supervision, Project administration, Methodology, Investigation, Funding acquisition, Formal analysis, Conceptualization.

Declaration of competing interest

The authors declare that they have no known competing financial interests or personal relationships that could have appeared to influence the work reported in this paper.

Acknowledgements

This research is funded by Hanoi University of Science and Technology (HUST) under project number T2023-PC-016 to SHN and the Fast-track grant of VinUniversity to MTT.

Appendix A. Supplementary data

Supplementary data to this article can be found online at https://doi.org/10.1016/j.heliyon.2024.e31617.

References

[1] B.V. Peechakara, H. Basit, M. Gupta, Ampicillin," StatPearls [Internet], StatPearls Publishing, Treasure Island (FL), 2023.
[2] D. KaushiK, M. Mohan, D.M. BoraDe, O.C. Swami, Ampicillin: rise fall and resurgence, J. Clin. Diagn. Res.: J. Clin. Diagn. Res. 8 (5) (2014) ME01, https://doi.org/10.7860/jcdr/2014/8777.4356.
[3] C. Manyi-Loh, S. Mamphweli, E. Meyer, A. Okoh, Antibiotic use in agriculture and its consequential resistance in environmental sources: potential public health implications, Molecules 23 (4) (2018) 795, 10.3390%2Fmolecules23040795.
[4] L. Serwecińska, Antimicrobials and antibiotic-resistant bacteria: a risk to the environment and to public health, Water 12 (12) (2020) 3313, https://doi.org/10.3390/w12123313.
[5] A.A. Chiș, et al., Microbial resistance to antibiotics and effective antibiotherapy, Biomedicines 10 (5) (2022) 1121, https://doi.org/10.3390/biomedicines10051121.
[6] R.C. Okocha, I.O. Olatoye, O.B. Adedeji, Food safety impacts of antimicrobial use and their residues in aquaculture, Publ. Health Rev. 39 (1) (2018) 1–22, https://doi.org/10.1186/s40985-018-0099-2.
[7] K. Pauter, M. Szultka-Młyńska, B. Buszewski, Determination and identification of antibiotic drugs and bacterial strains in biological samples, Molecules 25 (11) (2020) 2556, 10.3390%2Fmolecules25112556.
[8] S. Dawadi, et al., Technological advancements for the detection of antibiotics in food products, Processes 9 (9) (2021) 1500, https://doi.org/10.3390/pr9091500.
[9] S. Wang, B. Xu, Y. Zhang, J. He, Development of enzyme-linked immunosorbent assay (ELISA) for the detection of neomycin residues in pig muscle, chicken muscle, egg, fish, milk and kidney, Meat Sci. 82 (1) (2009) 53–58, https://doi.org/10.1016/j.meatsci.2008.12.003.
[10] R. Parthasarathy, C.E. Monette, S. Bracero, M.S. Saha, Methods for field measurement of antibiotic concentrations: limitations and outlook, FEMS Microbiol. Ecol. 94 (8) (2018) fiy105, https://doi.org/10.1093/femsec/fiy105.
[11] J. Hong, et al., A minireview for recent development of nanomaterial-based detection of antibiotics, Biosensors 13 (3) (2023) 327, https://doi.org/10.3390/bios13030327.
[12] M. Imran, et al., Nanostructured material-based optical and electrochemical detection of amoxicillin antibiotic, Luminescence 38 (7) (2023) 1064–1086, https://doi.org/10.1002/bio.4408.
[13] A.C.d.M. Mirres, et al., Recent advances in nanomaterial-based biosensors for pesticide detection in foods, Biosensors 12 (8) (2022) 572, https://doi.org/10.3390/bios12080572.
[14] M. Mahmoudpour, et al., Aptamer functionalized nanomaterials for biomedical applications: recent advances and new horizons, Nano Today 39 (2021) 101177, https://doi.org/10.1016/j.nantod.2021.101177.
[15] Y. Fan, et al., Detection of tetracycline antibiotics using fluorescent "Turn-off" sensor based on S, N-doped carbon quantum dots, Spectrochim. Acta Mol. Biomol. Spectrosc. 274 (2022) 121033, https://doi.org/10.1016/j.saa.2022.121033.
[16] D. Wei, et al., Quantum dot nanobeads based fluorescence immunoassay for the quantitative detection of sulfamethazine in chicken and milk, Sensors 21 (19) (2021) 6604, https://doi.org/10.3390/s21196604.
[17] Q.u.A. Zahra, Z. Luo, R. Ali, M.I. Khan, F. Li, B. Qiu, Advances in gold nanoparticles-based colorimetric aptasensors for the detection of antibiotics: an overview of the past decade, Nanomaterials 11 (4) (2021) 840, https://doi.org/10.3390/nano11040840.
[18] N.R. Tiwari, A. Rathore, A. Prabhune, S.K. Kulkarni, Gold nanoparticles for colorimetric detection of hydrolysis of antibiotics by penicillin G acylase, Adv. Biosci. Biotechnol. 1 (4) (2010) 322–329, https://doi.org/10.4236/abb.2010.14042.
[19] T. Li, G. Liu, H. Kong, G. Yang, G. Wei, X. Zhou, Recent advances in photonic crystal-based sensors, Coord. Chem. Rev. 475 (2023) 214909, https://doi.org/10.1016/j.ccr.2022.214909.
[20] S. Sadeghi, M. Jahani, F. Belador, The development of a new optical sensor based on the Mn doped ZnS quantum dots modified with the molecularly imprinted polymers for sensitive recognition of florfenicol, Spectrochim. Acta Mol. Biomol. Spectrosc. 159 (2016) 83–89, https://doi.org/10.1016/j.saa.2016.01.043.
[21] Z. Liu, J. Hou, Q. He, X. Luo, D. Huo, C. Hou, New application of Mn-doped ZnS quantum dots: phosphorescent sensor for the rapid screening of chloramphenicol and tetracycline residues, Anal. Methods 12 (27) (2020) 3513–3522, https://doi.org/10.1039/D0AY00961J.
[22] Z. Wang, Y. Zhang, B. Zhang, X. Lu, Mn2+ doped ZnS QDs modified fluorescence sensor based on molecularly imprinted polymer/sol-gel chemistry for detection of Serotonin, Talanta 190 (2018) 1–8, https://doi.org/10.1016/j.talanta.2018.07.065.
[23] C.P. Jiménez-Gómez, J.A. Cecilia, Chitosan: a natural biopolymer with a wide and varied range of applications, Molecules 25 (17) (2020) 3981, 10.3390%2Fmolecules25173981.
[24] S. Baruah, H. Warad, A. Chindaduang, G. Tumcharern, J. Dutta, Studies on chitosan stabilised ZnS: Mn2+ nanoparticles, J. Bionanoscience 2 (1) (2008) 42–48, https://doi.org/10.1166/jbns.2008.025.
[25] S. Wang, A fluorescent sensor based on one-step fabrication of chitosan/ZnS: Mn2+ composite film for iodine ion detection, Mater. Technol. 33 (4) (2018) 271–275, https://doi.org/10.1080/10667857.2017.1421038.
[26] S.H. Nguyen, P.K.T. Vu, H.M. Nguyen, M.T. Tran, Optical glucose sensors based on chitosan-capped ZnS-doped Mn nanomaterials, Sensors 23 (5) (2023) 2841 [Online]. Available: https://www.mdpi.com/1424-8220/23/5/2841.
[27] S.H. Nguyen, P.K.T. Vu, M.T. Tran, Glucose sensors based on chitosan capped Zns doped Mn nanomaterials, IEEE Sensors Letters 7 (2) (2023) 1–4, https://doi.org/10.1109/LSENS.2023.3240240.
[28] H. Wang, L. Wang, Y. Xiu, S. Zhang, S. Wang, X. Niu, Penicillin biosensor based on rhombus-shaped porous carbon/hematoxylin/penicillinase, J. Food Sci. 86 (8) (2021) 3505–3516, https://doi.org/10.1111/1750-3841.15841.
[29] A.R. Maheo, et al., Cytotoxic, antidiabetic, and antioxidant study of biogenically improvised elsholtzia blanda and chitosan-assisted zinc oxide nanoparticles, ACS Omega 8 (12) (2023) 10954–10967, https://doi.org/10.1021/acsomega.2c07530.
[30] H. Raghuram, S. Pradeep, S. Dash, R. Chowdhury, S. Mazumder, Chitosan-encapsulated ZnS: m (M: Fe3+ or Mn2+) quantum dots for fluorescent labelling of sulphate-reducing bacteria, Bull. Mater. Sci. 39 (2016) 405–413, https://doi.org/10.1007/s12034-016-1178-y.
[31] F. Li, et al., Detection limits of antibiotics in wastewater by real-time UV-VIS Spectrometry at different optical path length, Processes 10 (12) (2022) 2614, https://doi.org/10.3390/pr10122614.
[32] M. Hamami, M. Bouaziz, N. Raouafi, A. Bendounan, H. Korri-Youssoufi, MoS2/PPy nanocomposite as a transducer for electrochemical aptasensor of ampicillin in river water, Biosensors 11 (9) (2021) 311, https://doi.org/10.3390/bios11090311.
[33] Y. Lin, S. Cen, Content determination of ampicillin by Ni (ii)-mediated UV-Vis spectrophotometry, RSC Adv. 12 (16) (2022) 9786–9792, https://doi.org/10.1039/D2RA00116K.
[34] J.L. García-Zamora, J. Alonso-Arenas, G. Rebollar-Pérez, F.M. Pacheco-Aguirre, E. García-Diaz, E. Torres, Detection of ampicillin based on the fluorescence of a biocatalytic oxidation product, Front. Environ. Sci. 10 (2022) 2395, https://doi.org/10.3389/fenvs.2022.1040903.
[35] O.H. Shayesteh, R. Ghavami, Two colorimetric ampicillin sensing schemes based on the interaction of aptamers with gold nanoparticles, Microchim. Acta 186 (2019) 1–10, https://doi.org/10.1007/s00604-019-3524-4.
[36] H. Youn, et al., Aptasensor for multiplex detection of antibiotics based on FRET strategy combined with aptamer/graphene oxide complex, Sci. Rep. 9 (1) (2019) 7659, https://doi.org/10.1038/s41598-019-44051-3.